



HAL
open science

Development of a set of synthetic diagnostics for the WEST tokamak to confront 2D transport simulations and experimental data

Ivan Kudashev, Anna Medvedeva, Nicolas Fedorszak, David Zarzoso, Manuel Scotto d' Abusco, Vladislav Neverov, Pascal Devynck, Eric Serre

► To cite this version:

Ivan Kudashev, Anna Medvedeva, Nicolas Fedorszak, David Zarzoso, Manuel Scotto d' Abusco, et al.. Development of a set of synthetic diagnostics for the WEST tokamak to confront 2D transport simulations and experimental data. *Journal of Instrumentation*, 2023, 18 (02), pp.C02058. 10.1088/1748-0221/18/02/C02058 . hal-04010344

HAL Id: hal-04010344

<https://hal.science/hal-04010344v1>

Submitted on 1 Mar 2023

HAL is a multi-disciplinary open access archive for the deposit and dissemination of scientific research documents, whether they are published or not. The documents may come from teaching and research institutions in France or abroad, or from public or private research centers.

L'archive ouverte pluridisciplinaire **HAL**, est destinée au dépôt et à la diffusion de documents scientifiques de niveau recherche, publiés ou non, émanant des établissements d'enseignement et de recherche français ou étrangers, des laboratoires publics ou privés.

5 **Development of a set of synthetic diagnostics for the** 6 **WEST tokamak to confront 2D transport simulations** 7 **and experimental data**

8 **I. Kudashev,^{a,1} A. Medvedeva,^a N. Fedorszak,^b D. Zarzoso,^a M. S. d'Abusco,^a V.**
9 **Neverov,^c P. Devynck,^b E. Serre^a**

10 ^a*Aix-Marseille Université, CNRS, Centrale Marseille, M2P2 UMR 7340,*
11 *Marseille, France*

12 ^b*IRFM, CEA Cadarache,*
13 *13108 Saint Paul-lez-Durance, France*

14 ^c*National Research Centre "Kurchatov Institute",*
15 *Moscow, Russian Federation*

16 *E-mail: ivan.kudashev@univ-amu.fr*

17 **ABSTRACT:** Significant scientific effort has been focused on optimizing the scenarios and plasma pa-
18 rameters for tokamak operations. The lack of comprehensive understanding of underlying physical
19 processes leads to simplifications used both in plasma simulation codes and for diagnostics, which
20 is also complicated by the harsh plasma environment. One of the main tools to couple, check and
21 verify these assumptions are the synthetic diagnostics. In this work we demonstrate current results
22 of the development of the set of synthetic diagnostics for the WEST tokamak to couple experimental
23 data with the SolEdge3X-HDG 2D transport code.

24 **KEYWORDS:** Plasma diagnostics - interferometry, spectroscopy and imaging, Plasma diagnostics -
25 charged-particle spectroscopy

¹Corresponding author.

26 Contents

27	1 Introduction	1
28	2 Bolometer digital twin	1
29	2.1 Synthetic diagnostics and simulation parameters	1
30	2.2 Influence of wavelength resolved optic PFC model on bolometer signals	2
31	2.3 Bolometer signal tomographic inversions	3
32	3 Conclusions	4

33 1 Introduction

34 In order to improve and optimize tokamak performance, considerable scientific efforts have been put
35 into experimental and theoretical investigation of handling power and particle exhaust. However, the
36 harsh plasma environment complicates direct measurements and the interpretation of experimental
37 data remain challenging. Synthetic diagnostics might be very helpful in these circumstances
38 allowing confrontation between transport codes and the full set of plasma diagnostics.

39 In this work we demonstrate current results in the development of the set of synthetic diagnostics
40 for the WEST tokamak coupled with the SolEdge3X-HDG 2D transport code [1]. The numerical
41 models of the diagnostics exploit Cherab [2] and Raysect [3] Python libraries.

42 First results of this study, concerning horizontal bolometer system and synthetic visible camera
43 are shown in [4]. Here we focus more on the possibilities of the upcoming implementation of the
44 vertical bolometer systems. We evaluate influence of the reflections on the recorded signal using
45 wavelength resolved reflection models of plasma facing components (PFCs) and deuterium line
46 radiation in the range of bolometer detection. More detection channels also give an opportunity
47 to perform tomographic inversions of the detected radiation. We have performed first studies on
48 using conventional tomographic tool, non-negative least square (NNLS) solver, and an artificial
49 intelligence (AI) supplied one, variational autoencoder (VAE) and deep neural network (DNN).

50 2 Bolometer digital twin

51 2.1 Synthetic diagnostics and simulation parameters

52 A digital twin of bolometer systems of the WEST tokamak has been developed, which couples
53 2D plasma simulations using SolEdge3X-HDG code with the experimental data with the help of
54 Cherab and Raysect libraries. Deuterium 2D transport simulation of the entire WEST discharge
55 # 54487 was employed as a simulated plasma background, details of which can be found in [6].
56 Plasma radiation was calculated based on profiles $n_e, n_{D^+}, n_{D^0}, T_i, T_e$. To evaluate reflections
57 influence deuterium Lyman lines ($\alpha, \beta, \gamma, \epsilon$) has been taken into account using corresponding

58 photon emission coefficients from OpenADAS [7]. Fully absorbing and glossy tungsten models of
 59 the WEST PFCs has been compared as the most extreme cases. Refractive index and extinction
 60 coefficient were taken from [8].

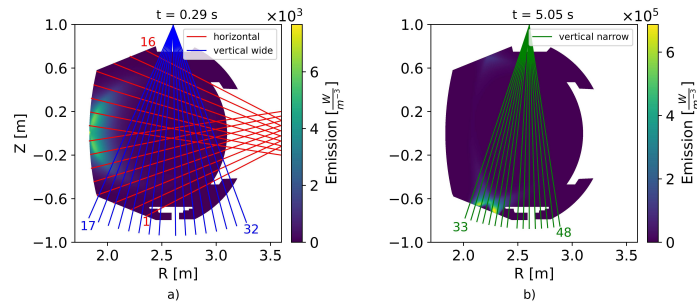


Figure 1. a) Radiation profile at the limiter stage of the discharge with horizontal and vertical wide bolometer LOSs; b) radiation profile at flat-top stage with vertical narrow bolometer LOSs

61 To create a training dataset of 64×64 pixel images of radiation for AI supported tomography
 62 inversion TotalRadiatedPower model from Cherab has been employed, based on approximately 400
 63 snapshots of the discharge under consideration. This model takes into account total continuum re-
 64 combination, line recombination and excitation and bremsstrahlung emission based on OpenADAS
 65 [7]. Pure deuterium plasma and fully absorbing PFC have been used. For these parameters dif-
 66 ference between TotalRadiatedPower and sum of chosen Lyman series lines of deuterium radiation
 67 was lower than few percents for considered discharge.

68 Lines of sights of bolometer systems with radiation profiles for limiter and flat-top discharge
 69 are shown in the figure 1. Details of the horizontal system are described in [4, 5]. Parameters of
 70 the foils of the horizontal cameras are similar, but 16 foils per each. Centers of the rectangular
 71 slits are located at $(R, Z, \phi) = (2.61 \text{ m}, 0.99 \text{ m}, 279.3^\circ)$, $(2.61 \text{ m}, 0.99 \text{ m}, 280.1^\circ)$ with their size
 72 of $4.3 \times 6.1 \text{ mm}$, $13 \times 6.1 \text{ mm}$, distance between slit and foils of 10.2, 16.7 cm correspondingly for
 73 "wide" and "narrow" vertical systems and distance between foils approximately 5 mm.

74 2.2 Influence of wavelength resolved optic PFC model on bolometer signals

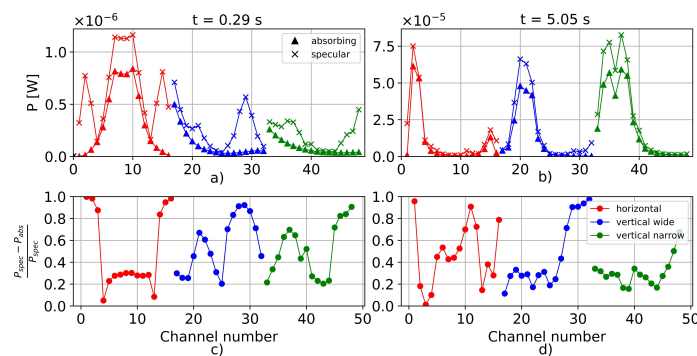


Figure 2. Simulated bolometer signals (a, b) for absorbing (triangles) and specular tungsten (crosses) models and their relative difference (c, d) for limiter (a, c) and flat-top (b, d) phases of the discharge

75 We calculated bolometer signals for limiter and flat-top phases from figure 1 for absorbing
 76 and specular tungsten models. According to figure 2 the reflected light can contribute up to almost
 77 100% of detected power. This difference is most noticeable for channels which do not cross the
 78 most radiating parts of the plasma but collect light due to reflections. These channels should be
 79 properly considered while interpreting experimental data. However, this extreme case of specular
 80 tungsten may be far from real surfaces which should be more diffusive. Nevertheless it is shown
 81 that reflections can play a significant role for bolometers in WEST tokamak.

82 2.3 Bolometer signal tomographic inversions

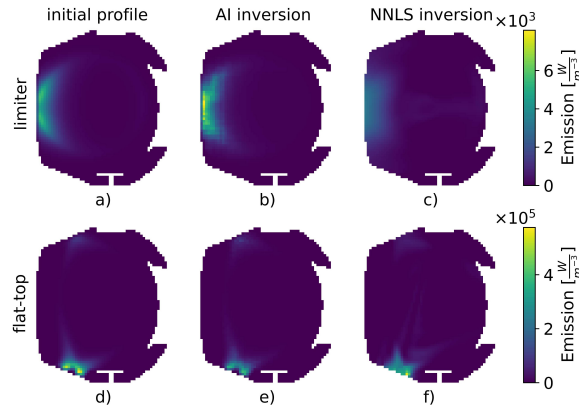


Figure 3. Tomographic inversions using AI (b, e) and NNLS method (c, f) of the initial profiles (a,d) for limiter (a, b, c) and flat-top (d, e, f) phases of the discharge

83 Using the synthetic diagnostic coupled with 2D plasma simulation we can investigate the
 84 possibilities of the tomographic inversions of the bolometer signals without having experimental
 85 data yet. We can provide radiation profiles such as in figure 1 and then obtain simulated bolometer
 86 signals. Inverting them, we can restore 2D profiles of radiation and compare with the initial one.

87 We used two methods of inversions. First, using Cherab methods for NNLS (non-negative least
 88 square solver) with ADMT (Anisotropic Diffusion Model Tomography) regularisation operator [9],
 89 implying the assumption that radiation should vary less along magnetic flux surfaces than across.
 90 For the second one we employed AI libraries Keras [10] and TensorFlow [11] to build Variational
 91 Autoencoder (VAE) which reproduces initial 2D profiles passing through a bottleneck of latent
 92 space, which is reduced information of the dataset profiles. VAE consisted of convolutional part of
 93 3 convolutional layers with MaxPooling and of deconvolutional part of 3 convolutional layers with
 94 UpSampling. Then a DNN with two dense layers was trained to connect 48 bolometer signals with
 95 16 values in the latent space of VAE. Radiation profiles and detected bolometer signals in training
 96 dataset were normalized to values in the range from 0 to 1, using logarithmic scale in the range of
 97 lowest and highest expected signals to be detected. After training bolometer signals can be passed
 98 through deep neural network (DNN) and decoder part of VAE to obtain 2D profiles of radiation.

99 According to figure 3 we can see that AI supported tomography gives slightly better results
 100 compared with NNLS which has some artifacts, caused by the use of sensitivity matrices. However,
 101 the AI tool might be overtrained on a given dataset and further studies with higher variety of
 102 phantoms for various magnetic profiles and sources of radiation should be done.

103 3 Conclusions

104 In this contribution we present the progress in the development of a set of synthetic diagnostics for
105 the WEST tokamak. Taking into account wavelength resolved plasma emission as well as applying
106 a PFCs surface model we showed that for deuterium plasmas reflections might contribute up to
107 100% of detected power, especially for the outer channels of the vertical bolometers. Expanding our
108 digital twin with vertical bolometer cameras allowed to perform tomography using VAE and DNN
109 and NNLS method. The inversions of a promising quality are achieved and further investigation on
110 different tomography methods, employing more variable sets of the phantoms of radiation, should
111 be performed.

112 Acknowledgments

113 This work has been supported by the French National Research Agency grant SISTEM (ANR-19-
114 CE46-0005-03). One of the authors (D.Z.) has received financial support from the AIM4EP project
115 (ANR-21-CE30-0018), funded by the French National Research Agency (ANR.).

116 References

- 117 [1] G. Giorgiani, et al., *A hybrid discontinuous Galerkin method for tokamak edge plasma simulations in*
118 *global realistic geometry.*, *J. Comput. Phys* **374** (2018) 515–532.
- 119 [2] M. Carr, et al., *Physically principled reflection models applied to filtered camera imaging inversions*
120 *in metal walled fusion machines.*, *Rev. Sci. Instrum* **90** (2019) 043504.
- 121 [3] A. Meakins and M. Carr, *Raysect Python Raytracing Package (Version v0.7.0)*. Available online:
122 <https://doi.org/10.5281/zenodo.4257023>.
- 123 [4] I. Kudashev, et al., *Development of a set of synthetic diagnostics for the confrontation between 2D*
124 *transport simulations and WEST tokamak experimental data.*, *Appl. Sci.* **12** (2022) 9807.
- 125 [5] P. Devynck, et al., *Calculation of the radiated power in WEST.*, *J. Phys. Commun.* **5** (2021) 095008.
- 126 [6] M. S. d' Abusco, et al., *Core-edge 2D fluid modeling of full tokamak discharge with varying magnetic*
127 *equilibrium: From WEST start-up to ramp-down.*, *Nuclear Fusion* **62** (2022) 08600.
- 128 [7] H. Summers *The ADAS User Manual, Version 2.6*. Available online: <http://www.adas.ac.uk/>
129 (2004).
- 130 [8] W. S. M. Werner, K. Glantschnig and C. Ambrosch-Draxl *Optical constants and inelastic*
131 *electron-scattering data for 17 elemental metals*, *J. Phys Chem Ref, Data* **38** (2009) 1013-1092.
- 132 [9] L. C. Ingesson *The mathematics of some tomography algorithms used at JET*, Abingdon, UK: JET
133 Joint Undertaking, (2000).
- 134 [10] F. Chollet, et al. *Keras*, <https://keras.io> (2015).
- 135 [11] M. Abadi, et al. *TensorFlow: a system for Large-Scale machine learning*, (2015) Software available
136 from <https://tensorflow.org>.